Structure and magnetic properties of RNi$_2$Mn compounds (R=Tb, Dy, Ho, and Er)

J. L. Wang,[1,2,3] C. Marquina,[2] M. R. Ibarra,[2] and G. H. Wu[1]
[1]*State Key Laboratory of Magnetism, Institute of Physics, Chinese Academy of Sciences, P.O. Box 603, Beijing 100080, People's Republic of China*
[2]*Departmento de Física de la Materia Condensada-Instituto de Ciencia de Materiales de Aragón, Universidad de Zaragoza-CSIC, Pedro Cerbuna 12, 50009 Zaragoza, Spain*
[3]*School of Physical, Environmental and Mathematical Sciences, University of New South Wales, The Australian Defense Force Academy, Canberra ACT 2600, Australia*
(Received 12 April 2005; revised manuscript received 19 January 2006; published 24 March 2006)

The compounds RNi$_2$Mn (R=Tb, Dy, Ho, and Er) with a MgCu$_2$-type structure have been synthesized. The R to transition metal atom ratio is confirmed to be 1:3 using the energy dispersive spectroscopy. The structural and magnetic properties have been investigated by various experimental methods. The x-ray diffraction patterns (XRD) can be well indexed with a cubic Laves cell and space group Fd3m. The refinement results of the XRD patterns show the presence of vacancies in the crystallographic structure. The ordering temperatures T_C have been derived to be 131, 94, 75, and 50 K for R=Tb, Dy, Ho and Er, respectively, which are much higher than those of their corresponding RNi$_2$ and RMn$_2$ compounds. A large difference of M-T curves between zero-field-cooling and field-cooling magnetization for all samples at a certain temperature range is observed in a low field, which can be understood in the terms of narrow-domain-wall pinning and a sensitive temperature dependence of coercivity.

DOI: 10.1103/PhysRevB.73.094436 PACS number(s): 75.30.Cr, 61.66.Dk, 75.50.Gg, 61.10.Nz

INTRODUCTION

It has been widely recognized that the study of rare-earth (R) transition-metal (T) intermetallic compounds can lead to the discovery of various functional materials.[1,2] In general, alloying 3d elements with R elements makes the magnetic moment of the 3d ions decrease with increasing the R-content. For example, in the R_xNi_y compounds the mean magnetic moment of Ni is strongly reduced with respect to the value of 0.6 μ_B in the pure metal: The mean magnetic moment per Ni atom is 0.16 μ_B in GdNi$_5$, 0.15 μ_B in GdNi$_3$, and 0.0 μ_B in GdNi$_2$ and GdNi.[3–6] All RNi$_2$ compounds crystallize in the cubic MgCu$_2$-type of laves phase structure (C15, space group Fd3m).[2] Recently, the compounds with the MgCu$_2$ structure have attracted interest again because some of them exhibit a large magnetocaloric effect.[7] The RMn$_2$ compounds crystallize either in the cubic C15 Laves-phase structure (for R=Y, Gd, Tb, and Dy) or in the hexagonal C14 Laves-phase structure (for R=Pr, Nd, Sm, Er, Tm, and Lu).[8,9] It has been reported that the variation in lattice parameters and magnetic properties across the R series is much more pronounced for the RMn$_2$ compounds than for the RNi$_2$ compounds. The magnetic ground state of the manganese atoms in the RMn$_2$ compounds depends critically on the R partner and on the Mn-Mn distance. In compounds with light R elements, where the Mn-Mn distance is above the critical distance 2.67 Å, the manganese atoms carry a moment 2 to 3 μ_B[10] whereas in compounds with R beyond Ho, with the Mn-Mn distances below 2.67 Å, the manganese moment disappears.[11] For DyMn$_2$, where the distance between the Mn atoms is close to the critical value, the Mn atoms do not have an intrinsic moment but have an induced magnetic moment on one-fourth of the Mn sites due to the strong molecular exchange field created by the spin-canted R sublattice.[12] With respect to the RT_3 intermetallics, most of the compounds with Fe, Co, and Ni crystallize in the rhombohedral PuNi$_3$-type of structure with space group R3m. The compounds exhibit a small spontaneous moment of about 0.05 μ_B per Ni atom and a low Curie temperature compared with the corresponding Fe and Co compounds.[2]

The partial substitution of the transition-metal element in the binary R_xT_y compounds by a different 3d metal is an effective method to study the magnetic interactions in the R-T compounds, their magnetic and structural properties and their dependence with the chemical composition, as well as for searching for novel compounds with outstanding magnetic properties. We have successfully synthesized RNi$_2$Mn compounds with R=Tb, Dy, Ho, and Er. In this article a detailed study of the structure and magnetic properties of these compounds is presented.

EXPERIMENTAL

The RNi$_2$Mn alloys with R=Tb, Dy, Ho, and Er were prepared by argon arc-melting the starting elements with purities of at least 99.9%. The constituents were melted in the stoichiometric amounts according to the 1:2:1 stoichiometry, plus an excess of Mn (less than 5%), to compensate the Mn evaporation during the arc-melting and the subsequent annealing processes. The x-ray powder diffraction (XRD) data were collected on a Rigaku Rint-2400 diffractometer working with Cu $K\alpha$ radiation and a graphite monochromator, using a scanning step of 2θ=0.02° and a sampling time of 2 s. The chemical composition of the Tb- and Dy-containing samples was checked by energy dispersive spectroscopy (EDS). The temperature dependence of the magnetization as well as the hysteresis loops were measured in a superconducting quantum interference device (SQUID) magnetometer and in an extraction-sample magnetometer.

TABLE I. Structural and magnetic parameters of RNi$_2$Mn, RNi$_2$, and RMn$_2$ compounds (the experimental error in the lattice parameter of the RNi$_2$Mn is ±0.001 Å).

Compounds	a (Å)	V (Å^3)	T_C (K)	Ms (μ_B/f.u.)	Ref.
TbNi$_2$Mn	7.185	370.9	131	4.8	this work
DyNi$_2$Mn	7.140	364.1	94	6.7	this work
HoNi$_2$Mn	7.135	363.4	75	7.4	this work
ErNi$_2$Mn	7.126	361.9	50	4.5	this work
TbNi$_2$	7.16	367.1	37.5	7.67	(9,15)
DyNi$_2$	7.142	364.3	22	9.23	(9,15)
HoNi$_2$	7.136	363.4	15	9.74	(9,15)
ErNi$_2$	7.1246	361.6	7	6.47	(9,15)
TbMn$_2$	7.635	445.1	54		(9,16)
DyMn$_2$	7.602	439.3	35	6.2[a]	(9,16,20)
HoMn$_2$	7.592	437.6	24	6.8[b]	(9,15,20)
ErMn$_2$	7.500	421.9	15		(9,16)

[a]Single crystal [111] direction.
[b]Single crystal [110] direction.

RESULTS AND DISCUSSION

The XRD patterns and thermomagnetic analysis show that the investigated RNi$_2$Mn samples are single phase with the MgCu$_2$-type structure, except for a small amount of impurity phase (detected at $2\theta=29^\circ$ in the cases of the HoNi$_2$Mn and ErNi$_2$Mn samples, and at $2\theta=24^\circ$ in the cases of TbNi$_2$Mn and DyNi$_2$Mn). The XRD patterns can be successfully indexed with a space group Fd3m. Therefore, the crystal structure of the RNi$_2$Mn compounds is the same as that of the RNi$_2$ intermetallics. The cubic lattice parameters at room temperature derived from the XRD patterns of powder samples are listed in Table I, together with those of the parent compounds RNi$_2$ and RMn$_2$. It can be seen that the unit cell volume decreases clearly with increasing the atomic number due to the lanthanide contraction. The lattice parameter and, therefore, the unit cell volume of the RNi$_2$Mn compounds are closer to those of the RNi$_2$ than to those of the RMn$_2$ parent compounds.

The obtained ingots were weighted after arc-melting and annealing, and the final weight was compared with the starting constituents total weight. The results confirm that the weight loss coincides in all the cases with the Mn loss. Therefore, we can assume that the 1:2:1 stoichiometry is preserved in the final sample. In order to further confirm the actual composition TbNi$_2$Mn and DyNi$_2$Mn were chosen to perform EDS experiments. The results for TbNi$_2$Mn are: Tb 25.3±0.6, Ni 51.2±0.6, and Mn 24.6±0.6, and for DyNi$_2$Mn: Dy 25.7±0.8, Ni 50.4±0.7, and Mn 23.9±0.7. These results have confirmed that the R/(NiMn) ratio is 1:3 within the experimental error.

Therefore, as the XRD patterns are clearly different from those of the compounds, there is a contradiction between the crystallographic structure and the chemical composition. In order to understand this discrepancy the refinement of the XRD patterns[13] has been performed by using the program FULLPROF.[14] It is known that the R and T atoms in RT_2 compounds with the MgCu$_2$-type of structure occupy the 8a and 16d sites, respectively.[2] In the present case a RNi$_2$ structure has been assumed in which there can be vacancies at the R sites. Some of these vacancies can be occupied by Mn atoms. To take this into account we have rewritten the chemical formula as $(R_{1+v}\mathrm{Mn}_x)(\mathrm{Ni}_2\mathrm{Mn}_{1-x})$ and let $(1+v+x)/(2+1-x)$ equal 1:2, where v stands for the number of vacancies at the R sites and x stands for the number of Mn atoms occupying 8a sites. In the case of the Tb compound it has been found that the best refinement has been obtained when $x=0.30$ and $v=0.05$ (in this case, the pattern factor, R_p, the weighted pattern factor, R_w and the expected pattern factor R_{exp} become 10.7%, 13.8%, and 6.25%, respectively). Therefore, we can conclude that in the TbNi$_2$Mn compound the 8a sites are not fully occupied by Tb atoms. About 3.7% of these sites are empty and Mn atoms occupy approximately 22.2%. This can be the reason why the lattice parameters of the RNi$_2$Mn compounds are so close to those of the RNi$_2$, even though 25 at % of Mn in excess is contained in the compounds. The best refinements for RNi$_2$Mn are shown in Fig. 1 and the results for the TbNi$_2$Mn compound are listed in Table II.

Figure 2(a) shows the temperature dependence of the magnetization measured on bulk samples of RNi$_2$Mn compounds with R=Tb, Dy, Ho, and Er, in an applied magnetic field of 0.05 T. Measurements have been performed increasing the temperature, after zero-field cooling (ZFC) and field cooling (FC) the samples from temperatures well above room temperature down to 1.5 K. It can be seen that the ZFC and FC magnetization curves exhibit irreversible behavior below a certain temperature, hereafter called freezing temperature, T_f, which is marked by arrows in the figure. In all the cases, a second anomaly is observed below 50 K, at T_a. The origin of both anomalies will be discussed in the next paragraphs.

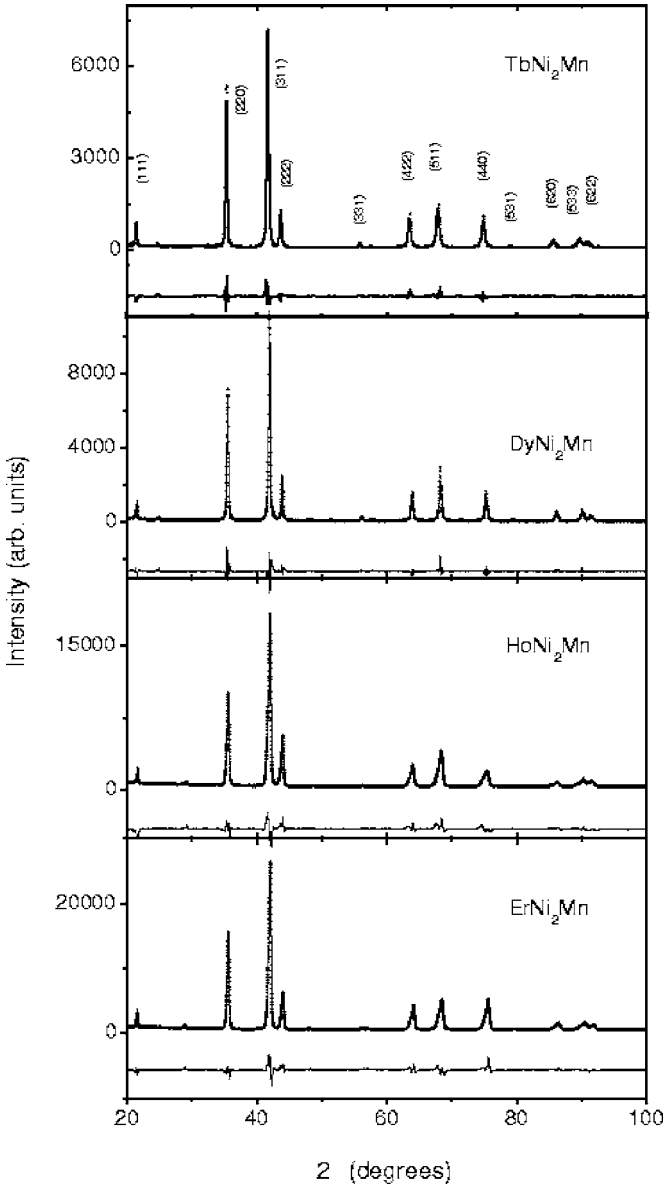

FIG. 1. XRD patterns of the RNi$_2$Mn compounds (R=Tb, Dy, Ho, and Er). Crosses indicate the observed data. The calculated profile obtained from Rietveld analysis corresponds to the continuous curve. The lower profile is the difference between the observed and calculated intensities at each angle step.

TABLE II. Rietveld-refinement results for the atomic positions and site-occupancy factor in a unit cell of the compound TbNi$_2$Mn [a=7.1581(8) Å, R_p=10.7%, R_w=13.8%, $R_{\exp}$=6.25%].

Atom	Positions	x/a	y/a	z/a	Site occupancy
Tb	8a	0	0	0	74.1%
Vacancy	8a	0	0	0	3.7%
Mn	8a	0	0	0	22.2%
Ni	16d	0.625	0.625	0.625	74.1%
Mn	16d	0.625	0.625	0.625	25.9%

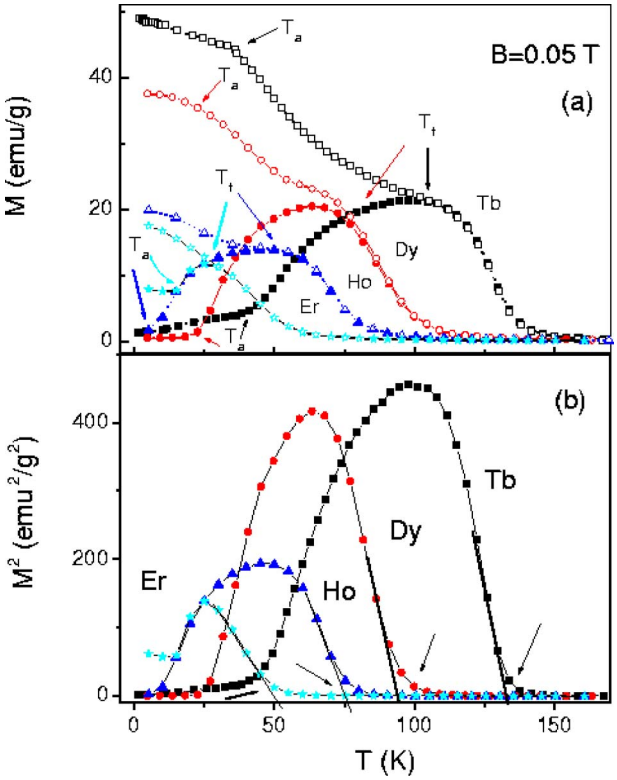

FIG. 2. (Color online) (a) Temperature dependence of the magnetization of RNi$_2$Mn compounds (R=Tb, Dy, Ho, and Er) in a field of 0.05 T after zero-field cooling (ZFC, solid symbols) and field cooling (FC, open symbols). (b) The square magnetization value as a function of temperature, obtained from the results plotted in (a). T_C is marked by arrows.

The Curie temperature, T_C, has been determined from M^2-T plots obtained from the M versus T measurements in an applied magnetic field of 0.05 T, by extrapolation of M^2 to zero [as shown in Fig. 2(b)]. The T_C values of RNi$_2$Mn are 131, 94, 75, and 50 K for R=Tb, Dy, Ho, and Er, respectively, which are clearly higher than the T_C values of the corresponding RNi$_2$ and RMn$_2$ compounds (listed in Table I[15,16]). As T_C is determined by the exchange interactions, the values in Table 1 suggest that the exchange interactions in RNi$_2$Mn are the strongest among these three series of compounds. The temperature dependence of the inverse magnetic susceptibility is shown in Fig. 3. The values of T_C derived from Fig. 3 are in good agreement with those derived from the M^2-T plots.

Figure 4 shows T_C as a function of the de Gennes factor, $G=(g-1)^2J(J+1)$, calculated for each R^{3+} ion (g is the Landé factor and J the quantum number of total angular momentum of R^{3+}). T_C of the parent RNi$_2$ and RMn$_2$ compounds is also drawn in the same figure for comparison. From the variation of T_C with the de Gennes factor it can be concluded that the exchange interaction in RNi$_2$Mn compounds is mainly attributed to the R-R exchange interaction, similar to the case in RNi$_2$ and RMn$_2$ compounds. In the insert of Fig. 4, T_C plotted versus the cubic lattice constant is shown. The T_C versus a curve can be easily understood, since the Ruderman-Kittel-Kasuya-Yusida (RKKY) interac-

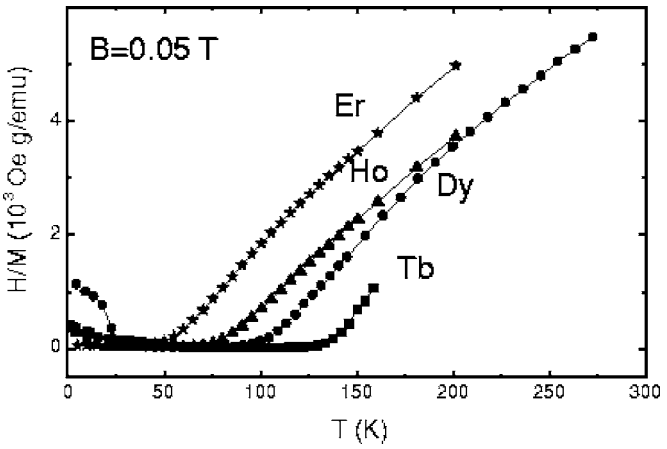

FIG. 3. Inverse magnetic susceptibility of RNi$_2$Mn compounds (R=Tb, Dy, Ho, and Er) as a function of the temperature, in a magnetic field of 0.05 T.

tion between the R moments is determined by both the magnitude of magnetic moment and the distance between rare earth ions.[16]

Irreversible temperature dependences of the magnetization as displayed in Fig. 2(a) can be ascribed either to a cluster glass behavior[17] or to magnetohistory effects resulting from the presence of narrow domain walls.[18,19] In order to elucidate their origin the ac susceptibility has been measured in the temperature range of 5–300 K, in an ac magnetic field of 4.5 Oe, varying the frequency from 10 to 100 Hz. The temperature dependences of the real and imaginary components of the ac susceptibility [$\chi'(T)$ and $\chi''(T)$, respectively] of the TbNi$_2$Mn bulk sample are shown in Fig. 5. A peak at about 130 K is observed, which corresponds to the onset of the magnetic order at T_C (similar to what was observed, for example, in the case of DyMn$_2$ and HoMn$_2$ single crystals[20,21]). An anomaly appears in the vicinity of T_a and T_f, as marked by arrows in the figure. It can also be seen that a change of the ac frequency does not change the shape of the $\chi'(T)$ and $\chi''(T)$ curves, which discards the spin glass hypothesis.

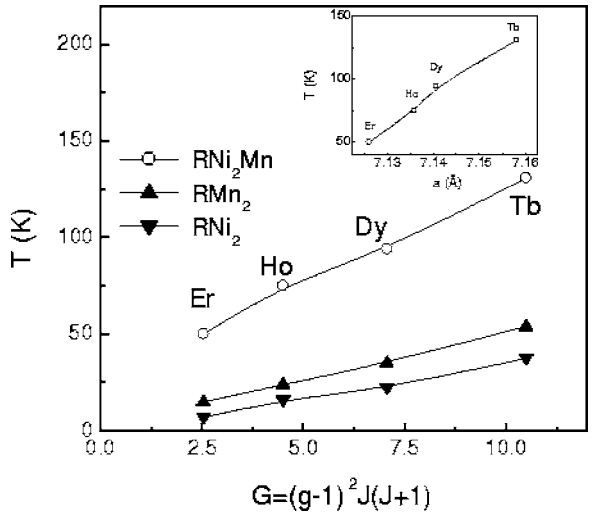

FIG. 4. Curie temperature, T_C, vs the de Gennes factor, $G=(g-1)^2J(J+1)$. Insert: T_C vs the lattice constant a.

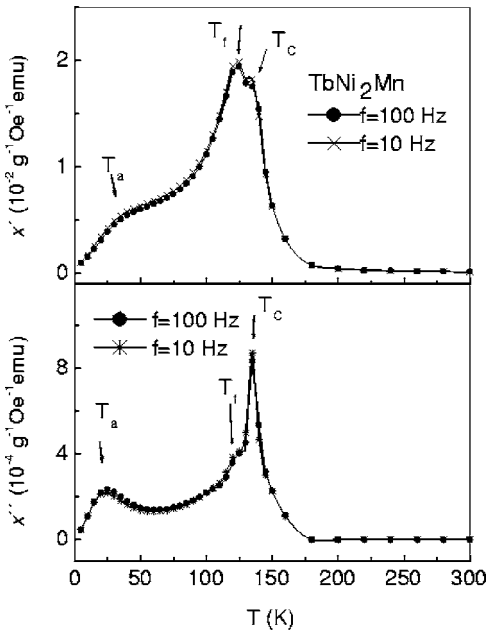

FIG. 5. AC magnetic susceptibility vs temperature performed applying an ac magnetic field of f=10 and 100 Hz for TbNi$_2$Mn bulk sample (upper panel: real part, χ'; lower panel: Imaginary part, χ'').

In order to explore the existence of magnetohistory effects as origin of the magnetization irreversibilities observed in the RNi$_2$Mn compounds, the magnetization vs. temperature measurements were performed varying the magnitude of the applied magnetic field. As an example, the temperature dependences of the magnetization after ZFC and FC in various applied fields for TbNi$_2$Mn are shown in Fig. 6. It can be seen that T_f, decreases with increasing the magnetic field. However, the irreversibility is observed even at large fields, as 2 T. On the contrary, the anomaly observed at T_a disappears as the magnetic field increases.

It is well known that for the ZFC process the magnetic domains are oriented in random directions when cooling the

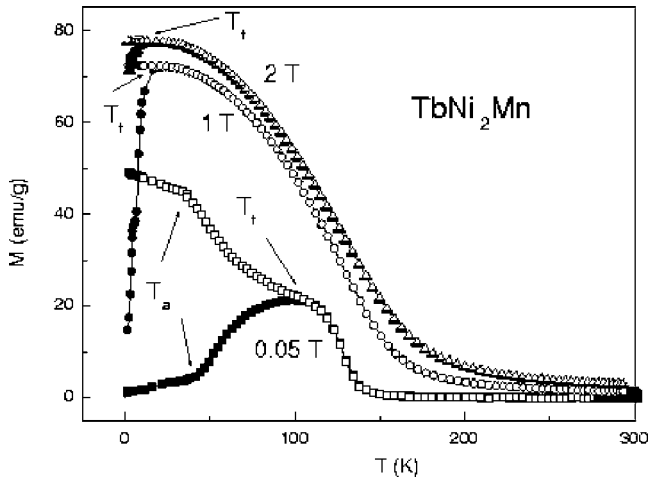

FIG. 6. Temperature dependence of the TbNi$_2$Mn magnetization in various magnetic fields after zero-field cooling (ZFC, solid symbols) and field cooling (FC, open symbols).

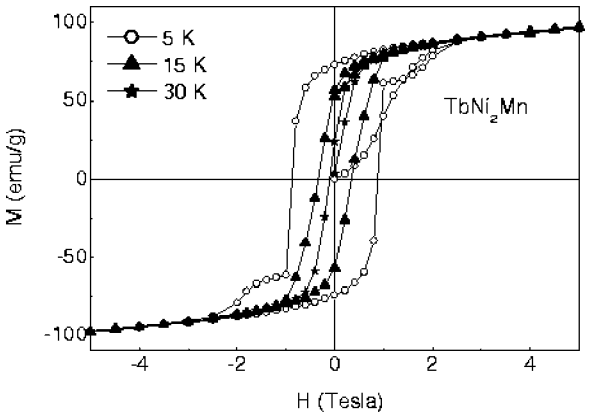

FIG. 7. Hysteresis loops of the $TbNi_2Mn$ bulk sample at 5, 15, and 30 K.

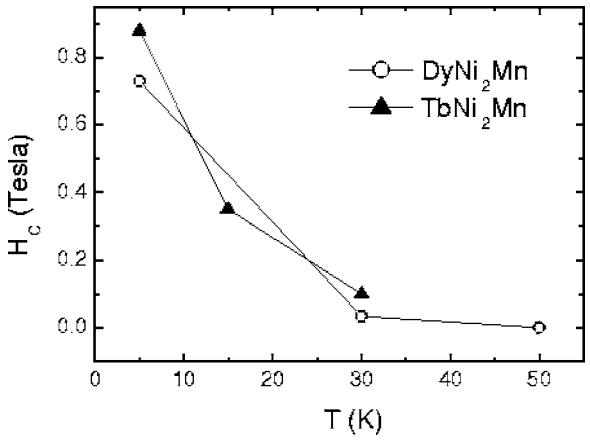

FIG. 8. Temperature dependence of the coercive field, H_C, for $TbNi_2Mn$ and $DyNi_2Mn$.

sample through T_C. When a small field is applied at 5 K, the magnetization of the sample is small because of a high coercivity at this temperature. As the temperature increases, the magnetic domain motion becomes easier due to the reduction of coercivity and, therefore, the magnetization increases. At a certain temperature, T_a, the coercivity decreases rapidly and the coercive field, H_C, becomes lower than the applied magnetic field. Therefore, the magnetic domain motion will accelerate suddenly, giving rise to an increase in the magnetization, which can be reflected in both M-T and $\chi'(T)$ $[\chi''(T)]$ curves.[22] For applied magnetic fields higher than H_C the anomaly at T_a is not observed. During the FC process, the initial magnetic state of the sample is different than after the ZFC process, because the magnetic domains are already oriented along the applied magnetic field direction, after cooling down the sample through T_C. As the domain walls move more easily when the temperature increases, the magnetization in the FC sequence is larger than that in ZFC case and the irreversibility at T_f occurs.

The magnetic hysteresis loop measurement is a useful and effective tool to study the magnetic domain motion.[22] Therefore, we performed the measurements for all the RNi$_2$Mn compounds at several temperatures. The hysteresis loops at 5, 15, and 30 K and the initial magnetization curve at 5 K of $TbNi_2Mn$ are shown in Fig. 7. A large magnetic hysteresis is observed at 5 K. The hysteresis loop is nearly square even though the sample is bulk polycrystalline. From the hysteresis loop a large coercive field H_C of 0.88 T at 5 K was obtained. The large magnetic hysteresis observed at low temperature on bulk specimens is entirely comparable to the cases of RCo$_{5-x}$Ni$_x$ with R=Y and La (Ref. 23) and $SmNi_4B$. (Ref. 24) With increasing temperature the coercivity of the bulk sample decreases quickly as shown in Fig. 7. The temperature dependence of coercivity for $TbNi_2Mn$ and $DyNi_2Mn$ compounds is shown in Fig. 8. A step-like increase of M is observed in the hysteresis loop at 5 K for $TbNi_2Mn$. The origin of this anomaly is not clear up to now and needs further investigation. Figure 9 draws the hysteresis loop and initial magnetization curve at 5 K for the other three bulk samples. It can be seen that the coercivity for the Ho and Er compounds is much smaller compared with that of the Tb and Dy compounds. It is well known that narrow-domain-wall pinning in homogeneous materials most likely takes place on obstacles of atomic dimensions. The presence of narrow domain walls requires a large ratio of the anisotropy energy to the exchange energy.[25] It has been reported that in $DyNi_2$ the anisotropy energy is very large. Even a field of 13.5 T applied along a hard magnetization axis cannot rotate the magnetization into the direction of the magnetic field.[5] Based on crystallographic considerations, it seems reasonable to assume that $DyNi_2Mn$ also has a large anisotropy. On

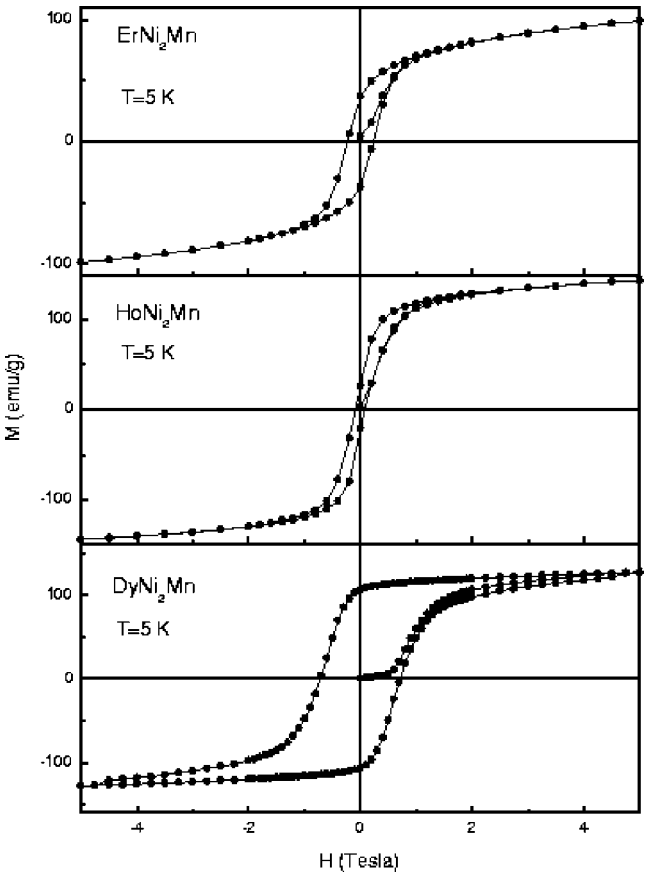

FIG. 9. Hysteresis loops and initial magnetization curve at 5 K of RNi$_2$Mn with R=Er, Ho, and Dy.

the other hand, the rather low Curie temperature of $DyNi_2Mn$ indicates that the exchange interaction is quite weak. Therefore, the necessary conditions for narrow-domain-wall formation can be satisfied in this system. The values of the spontaneous magnetization, M_s, of the RNi_2Mn compounds at 5 K have been obtained from the saturated part of *M-H* plots by extrapolating *H* to zero. For the compounds with R=Tb, Dy, Ho, and Er, M_s equals 4.8, 6.7, 7.4, and 4.5 μ_B/f.u., respectively. As it can be seen in Table I, the spontaneous magnetization of RNi_2Mn is smaller compared to that of the RNi_2 compounds. This fact indicates that the *T* sublattice in the RNi_2Mn compounds has a larger contribution to the total magnetic moment, since the coupling between the rare earth and transition-metal sublattice magnetizations is antiparallel in the *R-T* intermetallics with heavy *R* elements.[26] Assuming that the contribution from the Ni atoms to the magnetic moment is rather negligible, as in both the RNi_2 and compounds,[2–4] the low-temperature Ms values of the RNi_2Mn series suggest that the Mn atoms have a rather large magnetic moment in these compounds.

CONCLUSION

Compounds RNi_2Mn with R=Tb, Dy, Ho, and Er have been successfully synthesized. They show to crystallize in the $MgCu_2$-type of structure. It has been found that 74% of the 8*a* sites (R sites) are occupied by *R* atoms, Mn atoms occupy 22% and 4% are empty. RNi_2Mn shows ferrimagnetic *R*-Mn coupling with ordering temperatures much higher than the ordering temperatures of the RNi_2 and RMn_2 compounds. The values of the spontaneous magnetization of RNi_2Mn at 5 K suggest a rather large magnetic moment of the Mn atoms. Magneto-history effects and large coercive fields at 5 K in bulk samples (0.88 and 0.73 T for $TbNi_2Mn$ and $DyNi_2Mn$, respectively) are detected for all the samples, which can be quite well understood in terms of the narrow-domain-wall pinning and the sensitive temperature dependence of coercivity. These novel compounds represent the first of new family of intermetallic *R-T* compounds with the $MgCu_2$-type structure with these interesting magnetic phenomena, which deserve further exploration.

[1] K. H. J. Buschow, Rep. Prog. Phys. **40**, 1179 (1977).
[2] J. J. M. Franse and R. J. Radwanski, *Handbook of Magnetic Materials*, edited by K. H. J. Buschow (Elsevier Science, B.V., Amsterdam, 1993), Vol. 7, p. 307.
[3] D. Gignoux, D. Givord, and A. del Moral, Solid State Commun. **19**, 891 (1976).
[4] D. Gignoux, R. Lemaire, P. Mohlo, and F. Tasset, J. Magn. Magn. Mater. **21**, 307 (1980).
[5] D. Gignoux and F. Givord, Solid State Commun. **21**, 499 (1977).
[6] S. Jaakola, S. Parviainen, and S. Penttilä, J. Phys. F: Met. Phys. **13**, 491 (1983).
[7] F. W. Wang, X. X. Zhang, and F. X. Hu, Appl. Phys. Lett. **77**, 1360 (2000).
[8] M. Shiga, Physica B & C **149B**, 293 (1988).
[9] A. V. Morozkin, Yu. D. Seropeign, A. V. Gribanov, and J. M. Barakatova, J. Alloys Compd. **256**, 175 (1997).
[10] K. Yoshimura and Y. Nakamura, J. Magn. Magn. Mater. **40**, 55 (1983).
[11] H. Wada, H. Nakamura, E. Fukami, K. Yoshimura, M. Shiga, and Y. Nakamura, J. Magn. Magn. Mater. **70**, 55 (1987).
[12] C. Ritter, S. H. Kilcoyne, and R. Cywinski, J. Phys.: Condens. Matter **3**, 727 (1991).
[13] H. M. Rietved, Acta Crystallogr. **229**, 151 (1967).
[14] J. Rodríguez-Carvajal, Physica B **192**, 22 (1993).
[15] M. R. Ibarra, J. I. Arnaudas, P. A. Algarabel, and A. Del Moral, J. Magn. Magn. Mater. **46**, 167 (1984).
[16] K. Inoue, Y. Nakamura, A. V. Tsvyashchenko, and L. Fomicheva, J. Phys. Soc. Jpn. **64**, 2175 (1995).
[17] C. Christides, A. Kostikas, G. Zouganelis, V. Psyharis, X. C. Kou, and R. Grossinger, Phys. Rev. B **47**, 11220 (1993).
[18] J. L. Wang, Y. P. Shen, C. P. Yang, N. Tang, B. Fuquan, D. Yang, G. H. Wu, and F. M. Yang, J. Phys.: Condens. Matter **13**, 1733 (2001).
[19] T. H. Jacbos, K. H. J. Buschow, R. Verhoef, and F. R. de Boer, J. Less-Common Met. **157**, L11 (1990).
[20] E. Talik, M. Kulpa, T. Mydlarz, J. Kusz, and H. Böhm, J. Alloys Compd. **308**, 30 (2000).
[21] E. Talik, M. Kulpa, A. Winiarski, T. Mydlarz, and M. Neumann, J. Alloys Compd. **316**, 51 (2001).
[22] Z. R. Yang, S. Tan, and Y. H. Zhang, Appl. Phys. Lett. **79**, 3645 (2001).
[23] H. Oesterricher, F. T. Parker, and M. Misroch, Solid State Commun. **19**, 539 (1976).
[24] Chandan Mazumdar, R. Nagarajan, L. C. Gupta, B. D. Padalia, and R. Vijayaraghavan, Appl. Phys. Lett. **77**, 895 (2000).
[25] J. J. Vandenbroek and H. Zijlstra, IEEE Trans. Magn. **7**, 226 (1971).
[26] I. A. Campbell, J. Phys. F: Met. Phys. **2**, L47 (1972).